

Fast elastic full waveform inversion for microseismic location and focal mechanism

Xiong Zhang^{*1,2}, Jie Zhang¹, Mark D. Zoback²

¹University of Science & Technology of China (USTC), ²Stanford University

Summary

A fast elastic full waveform inversion method is developed to simultaneously find the global optimized solution for the locations and focal plane mechanisms of microseismic events. Given a velocity model, we first calculate synthetic Green's functions in a grid and create a database. We then extract a source wavelet from the input data to generate synthetic waveforms for calculating an approximate discrete objective function. Fast computation of synthetic seismograms with the Green's function database allows using Neighborhood Algorithm to determine the global minimum in a computationally efficient manner. The method applies an envelope cross-correlation approach to match high-frequency waveforms, thus, it requires event detection, but no accurate time picking needed. This method can effectively circumvent the issues of high frequency, low-amplitudes and high-resolution encountered analysis of microseismic data. We apply the method to 150 microseismic events obtained during hydraulic fracturing operations in the Barnett shale. The microseismic events were recorded in two wells. These events form several clusters and their source focal mechanisms indicate consistent fault orientations.

Introduction

Microseismic locations and focal plane mechanisms play an important role in understanding the fracture geometry and growth during hydraulic fracturing operations (Warpinski, 2009; Baig and Urbancic, 2010). The dynamic progress and the efficacy of the hydraulic fracturing can be estimated if one could determine the location and source focal mechanisms in real-time as stimulation was occurring. Most microseismic location methods utilize the traveltimes information of the direct P and S waves to determine 2D location of the events and then determine the azimuth of the location through the polarization of P waves (Warpinski, 2009). These methods involve picking arrival times (Warpinski, 2009). However, a single hydraulic fracturing stage frequently triggers hundreds to thousands of events with very low magnitudes, typically M-1 to -3. Thus, picking arrival times is often a difficult task. To avoid picking arrival times, several studies developed automatic migration-based methods to determine event locations (Rentsch et al., 2010; Haldorsen et al., 2012; Eaton et al., 2011).

Estimating reliable focal plane mechanisms is also a challenge in microseismic monitoring. A common practice

is to determine event locations first, and then calculate focal mechanisms. However, such strategies may produce focal mechanism solutions that are highly dependent on the accuracy of event locations (Kim, 2011). In earthquake seismology, Guilhem and Dreger (2011) perform linear moment-tensor inversions over a set of grids with pre-calculated Green's functions; Tsuruoka et al. (2009) solve a waveform grid search problem with long-period data. Zhang et al. (2014b) developed a search engine method that can very rapidly determine both source locations and source focal mechanism with long-period data recorded at three seismic stations. High-frequency and low-amplitude data and high-resolution requirements present serious challenges to these methods when dealing with microseismic problems.

Applying the elastic full waveform inversion method to simultaneously solve event for event locations and focal mechanism is another effort to solve these problems (Michel and Tsvankin, 2013; Zhang et al., 2014a). In addition to the direct P- and S-wave phases, other phases (such as reflections and converted waves) all contribute to the determination of location and focal mechanism (Zhang et al., 2014a). Zhang et al. (2014a) implement an elastic full waveform inversion for inverting both location and source focal mechanism based on a gradient-based optimization method. However, the gradient-based optimization method may suffer from the local minimum problem because of nonlinearity of the full waveform inversion. A global optimization algorithm might be able to deal with the nonlinear problem, but it would likely require hundreds to thousands of elastic waveform simulations. In this study, we use a discrete approximated objective function based on a precomputed Green's function database. We take both source focal mechanism and event location as the model space of the inversion and apply a neighborhood algorithm to invert them simultaneously. The neighborhood algorithm is a global optimization approach, and is a derivative-free search method.

Method

This method includes two steps to find the global minimum of the event location and source focal mechanism. We first build a large Green's function database for the area where the events potentially occur. Thus, all the possible elastic full waveforms can be synthesized based on the database without calculation of the Green's function during inversion. Then, a neighborhood algorithm is used to

Database based inversion for microseismic location and focal mechanism

invert for an event location and source focal mechanism simultaneously with the discrete approximation of the objective function (Sambridge, 1999). The objective function should be continuous for the traditional inversion method. However, we may need to approximate the continuous objective function using a discrete one because of the discrete Green's function database.

(a) Creating Green's function database

The most time consuming part of seismograms synthesis is the calculation of Green's function. We apply the General Reflection and Transmission Method (GRTM) to synthesize the Green's function in the 1D velocity model (Zhang et al., 2003). The Green's function is related to the horizontal distance between source and receiver and depth according to the symmetry in a cylindrical coordinate system. We assume that all the events during the hydraulic fracturing operation possibly occur in the horizontal distance range $[r_0, r_0 + m_r \Delta r]$ and the depth range $[z_0, z_0 + m_z \Delta z]$ for one of the receivers. The radius and depth are discretized with the intervals of Δr and Δz . Then we have the corresponding Green's function database as following.

$$\left\{ \begin{array}{l} G_{n,p}(r_i, z_j, t) | i = 0, 1, 2, \dots, m_r, \text{ and } j = 0, 1, 2, \dots, m_z \\ r_i = r_0 + i \Delta r, z_j = z_0 + j \Delta z \end{array} \right\}, \quad (1)$$

Where r_i are the discrete horizontal distance between the receiver and the source; z_j is the discrete depth of source;

$G_{n,p}(r_i, z_j, t)$ represents the Green's function at the location grid (r_i, z_j) . The total number of grids is $m_r \times m_z$. We calculate the Green's function at each grid to build a large Green's function database before inversion using the GRTM method. The Green's function database can be used as the input to a large number of event location and focal mechanism determination.

(b) Discrete approximation of the objective function

The elastic full waveform simulation is needed to calculate the value of the objective function during the inversion. Since Green's functions are ready, we just need to convolve the source radiation pattern with the Green's function as following.

$$\left\{ \begin{array}{l} u_n(m, t) \approx G_{n,p}(r_i, z_j, t) * \mathfrak{R}_p(\varphi, \lambda, \delta, \gamma, t) \\ m = (x, y, z, \lambda, \delta, \gamma), \varphi = \arctan(x/y) \\ r_i \approx \sqrt{x^2 + y^2}, z_j \approx z \end{array} \right. \quad (2)$$

where the model space m contains source location (x, y, z) in Cartesian coordinate and the source mechanism parameters. A double couple source focal mechanism is assumed with strike λ , dip δ , and rake γ . The displacement $u_n(m, t)$ can be approximated by the convolution between the Green's function in the database and the horizontal radiation pattern $\mathfrak{R}_p(\varphi, \lambda, \delta, \gamma, t)$. Because the location in terms of horizontal distance and depth is

discrete in the Green's function database, for any given location (x, y, z) , the displacement $u_n(m, t)$ can be estimated by the Green's function of which the discrete point (r_i, z_j)

is the vicinity of the given location $(\sqrt{x^2 + y^2}, z)$. If we choose the intervals Δr and Δz small enough, the approximation should be valid because resolution of the location is always finite. We use the above forward modeling Equation (2) in the following objective function as an example to implement the idea (Zhang et al., 2014a).

$$\left\{ \begin{array}{l} \psi(m) = \sum \|d_{obs}(t) - u_n(m, t, \Delta t)\|^2 \\ f(m, \tau) = \sum \int \tilde{d}_{obs}(t - \tau) \tilde{u}_n(m, t, 0) dt \\ \Delta t = \max_{\tau} f(m, \tau) \end{array} \right. \quad (3)$$

where $d_{obs}(t)$ is the observed data; $u_n(m, t, \Delta t)$ is the synthetic data with time shift Δt because of the unknown origin time. The time shift Δt can be calculated from the crosscorrelation between the envelopes of synthetic data and the real data as the function $f(m, \tau)$ shows after event detection. More details refer to Zhang et al. (2014a). In this study, the objective function is estimated by the discrete approximation as shown in Equation 2.

(c) Neighborhood algorithm (NA)

We use a global optimization method, the Neighborhood algorithm (NA) to minimize the objective function as shown by Equation 3 (Sambridge, 1999). Our model space includes locations and source focal mechanisms. The NA method includes four steps: (1) Generate an initial set of n_s models uniformly in the model space; (2) Calculate the value of the objective function (Equation 3) for the n_s models, then the n_r models with the lowest value are selected; (3) Generate n_s new models in the Voronoi cell of each of the n_r selected models (i.e. n_s/n_r samples in each cell); (4) Go to step 2. The Voronoi cell depicts the nearest neighbor region about one of the sampled models. The n_r should be less than n_s since we need to generate n_s/n_r models in each Voronoi cell. We avoid calculating the value of the objective function (Equation 3) throughout the whole parameter space as what grid search method does.

Synthetic example

To validate the performance of the algorithm, we apply the method to a synthetic example. The receiver geometry and the velocity model are taken from a real data example. The input waveforms are calculated using GRTM method in the same way as the Green's function database creation. A vertical receiver array and a deviated receiver array are deployed as shown in Fig. 1b (triangles). To construct the Green's function database, we assume that the induced fractures occur in the range from 1273.9 m to 1738.9 m in x direction, from 635.2 m to 940.0 m in y direction and 1807.2 m to 1990.1 m in depth. The Green's functions for each receiver are calculated separately with the horizontal and depth interval of 3 m in the model. We prepare an input waveform through convolution between the Green's function at the location (1500, 600, 1900) m and a double

Database based inversion for microseismic location and focal mechanism

couple source with strike 150° , dip 30° , rake 30° . A Ricker wavelet source time function with the center frequency of 66 Hz is selected.

As we are using the Neighborhood Algorithm to minimize the objective function, we can obtain a group of solutions including the best one. Fig 1 shows the inversion results of the synthetic example with the input waveform synthesized with GRTM method. Both the direct P and S waves and other seismic phases of the best-fitting solution match the input waveform very well (Fig. 1a). Other seismic phases may also be helpful to determine the location and source

focal mechanism especially in the single well case (Zhang et al, 2014a). Fig 1b shows that the method can well recover the true solution with event location and source focal mechanism. Fig. 1c shows the locations of 3100 models sampled by neighborhood algorithm. The dense area is the position where the solution is the most likely located. Most of the locations are around the true location as shown in Fig. 1c. As we calculate the synthetic waveform through the prepared the Green's function database. We can finish the waveform simulation of 3100 models with about 2.5 minutes in a single CPU (Intel (R) E5-2660).

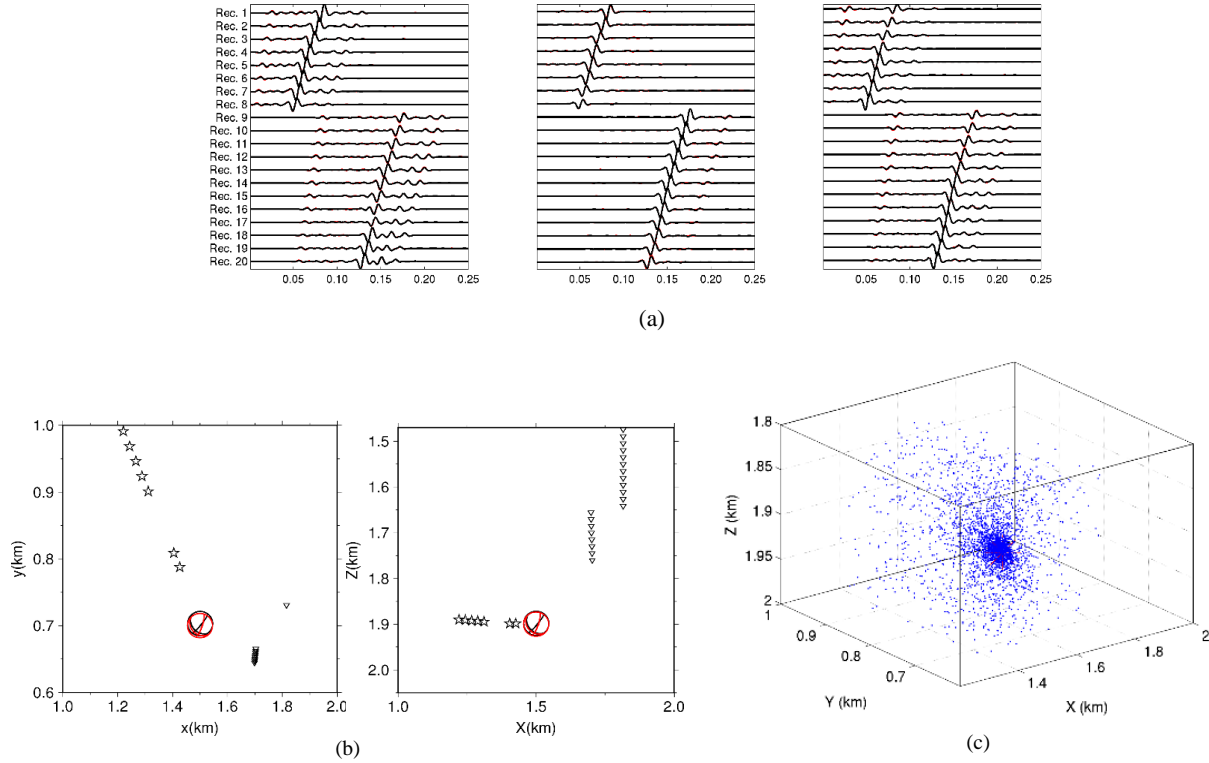


Figure 1. Synthetic example. The geometry and the velocity model are from the real data but the input waveform are synthesized using GRTM method in the same way as creating the Green's function. (a) Waveform overlay (X, Y, Z components) between the input waveform (red) and the synthetic waveform (black). (b) The true solution (red) and best solution (black). The red stars denote the perforation shots and triangles denote the receiver array. The locations for the true and best solutions are almost the same. (c) The distribution of 3100 solutions. The red star denotes the true location.

Real data example

There are a total of 150 events selected to test the performance of the proposed inversion scheme. The receiver arrays and velocity model are the same as in the synthetic example but the input is for real data with a bandpass filter from 0 to 200 Hz applied. Because the event waveform may be contaminated by the tube waves, the data with frequency below 200 Hz are useful for the inversion (Eisner et al, 2011).

Fig. 2 shows the inversion results for the 150 events. The source focal mechanisms seem similar among those located at the close positions. There are several event clusters

located from 1900 m to 2000 m in depth with similar source focal mechanisms. To validate the location results, we choose a reference event located at (1688.8, 708.5, 1962.1) m to compare synthetic and real waveform overlay as shown in Fig. 3a. The synthetic waveform can match the real data waveform well although the P wave is quite weak. In this particular case, it is very hard to determine the onset and polarization of the P wave if we were to use a traveltime-based location method. Fig. 3b shows the full waveform overlay of 5 close events around the reference event at the location (1688.8, 708.5, 1962.1) m with similar source focal mechanism as shown in Fig. 3c. Indeed the waveforms of these events are nearly identical, suggesting the similar fracturing process repeated at probably the same location.

Database based inversion for microseismic location and focal mechanism

Conclusions

We propose a discrete approximation for the objective function based on a precomputed Green's function database for the microseismic location and focal mechanism inversion problem. The synthetic waveform calculation is quite fast with this approximation based and the precomputed database of Green's function so that the global optimization method can be used in the elastic full waveform inversion of the microseismic data.

Possible improvements include: Use of other kinds of global optimization methods to be combined with the discrete approximation of the objective function. The source time function is also an issue for further consideration. We use a constant source time function for

the inversions. An accurate wavelet for the input data needs to be estimated. We can also optimize the central frequency of the wavelet during inversion. We assume the source to be a double-couple type in this study but some studies suggested that the events could be the results of opening cracks during hydraulic fracturing. Thus, the non-double couple focal mechanism should be considered with more independent parameters to depict the source focal mechanism. This warrants further studies.

Acknowledgement

We appreciate GeoTomo for the support for this research, and allowing us to use MiVu™ software package to do the tool orientation.

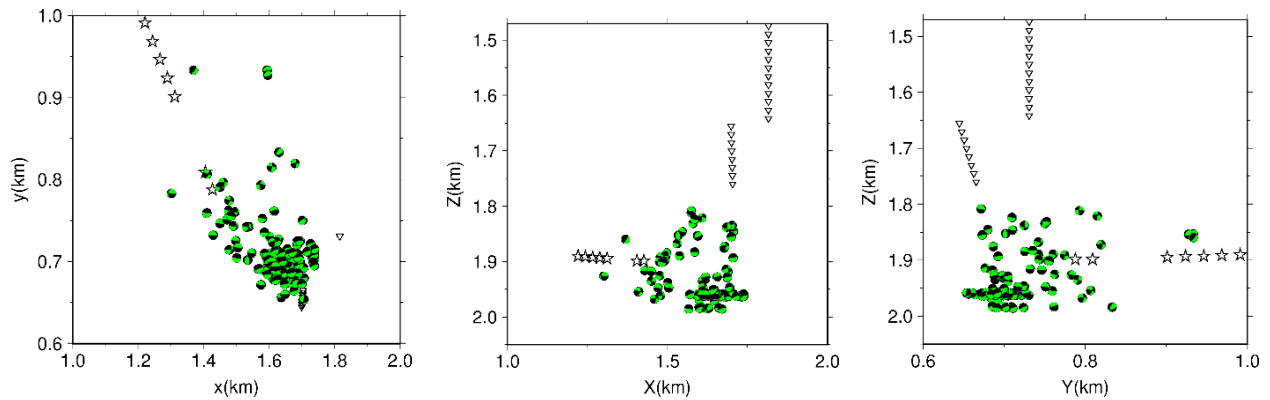


Figure 2. Inversion results for the 150 real data examples. The geometry and the velocity model are as the same as the one in synthetic example.

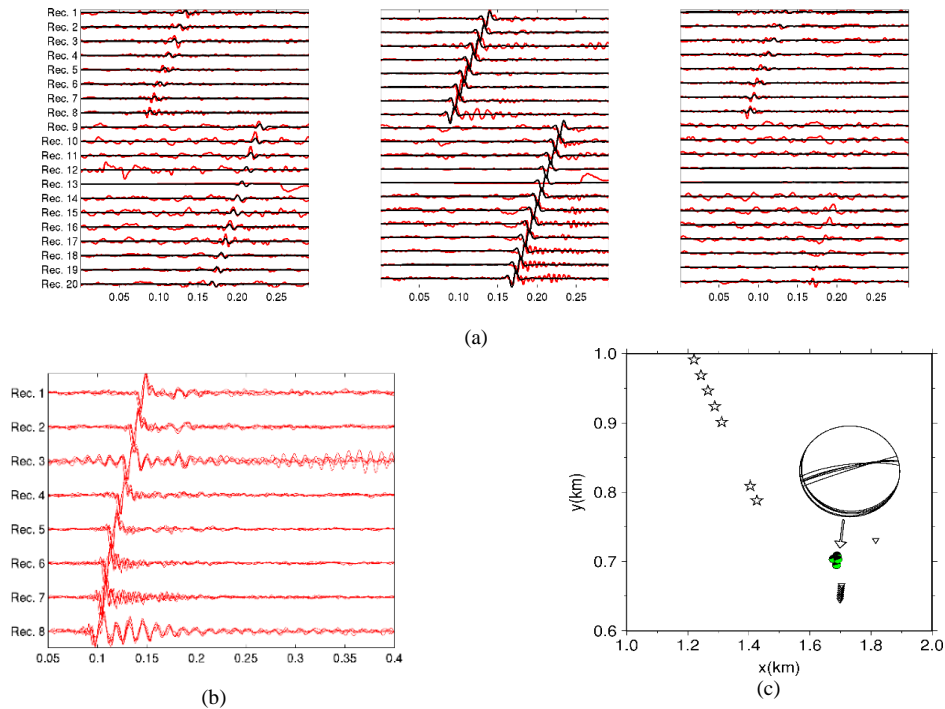


Figure 3. Waveform overlays and result comparisons. (a) The synthetic (black) and real (red) data waveform overlay for a reference event located at (1688.8, 708.5, 1962.1) m. (b) The waveform overlay of the y components of the event cluster near the referenced event as shown in Fig. 3c. (c) The location and focal mechanism for the event cluster.